Hierarchical Bayesian Modelling of Visual Attention

Jinhua Xu
Department of Computer Science and Technology, East China Normal University,
500 Dongchuan Road, Shanghai 200241, China

Keywords: Visual Attention, Visual Saliency, Bayesian Modeling, Object Localization.

Abstract: The brain employs interacting bottom-up and top-down processes to speed up searching and recognizing visual targets relevant to specific behavioral tasks. In this paper, we proposed a Bayesian model of visual attention that optimally integrates top-down, goal-driven attention and bottom-up, stimulus-driven visual saliency. In this approach, we formulated a multi-scale hierarchical model of objects in natural contexts, where the computing nodes at the higher levels have lower resolutions and larger sizes than the nodes at the lower levels, and provide local contexts for the nodes at the lower levels. The conditional probability of a visual variable given its context is calculated in an efficient way. The model entails several existing models of visual attention as its special cases. We tested this model as a predictor of human fixations in free-viewing and object searching tasks in natural scenes and found that the model performed very well.

1 INTRODUCTION

Human and many other animals have a remarkable ability to interpret complex scenes in real time, despite the limited information-processing speed of the neuronal hardware available for this task. Intermediate and higher visual processes appear to select a subset of the incoming sensory information for further processing. The most important function of selective visual attention is to direct our gaze rapidly towards objects of interests in our visual environment. There are two major categories of factors that drive attention: bottom-up (BU) factors and top-down (TD) factors. Bottom-up factors are derived solely from the incoming visual stimuli. Regions of interest that attract our attention in a bottom-up way are deemed salient and the visual features for this selection must be sufficiently discriminative with respect to the surrounding features. On the other hand, top-down attention is driven by cognitive factors such as knowledge, expectations, and current goals (Borji and Itti, 2013).

Computational models of visual attention have been extensively researched (see (Frintrop et al., 2010; Toet, 2011) for reviews). Over the past decade, many different algorithms have been proposed to model bottom-up visual saliency. They can be broadly classified as biologically-based (Itti et al., 1998), purely computational, or a combination of both(Bruce and Tsotsos, 2009). In Itti et al's model (Itti et al., 1998), a measure of saliency is computed based on the relative difference between a target and its surround along a set of feature dimensions (i.e., color, intensity, orientation, and motion). Several statistical models of visual saliency have also been developed (Bruce and Tsotsos, 2009; Zhang et al., 2008; Gao and Vasconcelos, 2009; Itti and Baldi, 2009). In these models, a set of statistics or probability distributions (PDs) of visual variables are computed from either the scene the subject is viewing or a set of natural scenes, and a variety of measures of visual saliency are defined on these statistics or PDs, including self-information (Bruce and Tsotsos, 2009; Zhang et al., 2008), discriminant power (Gao and Vasconcelos, 2009), Bayesian surprise (Itti and Baldi, 2009).

For top-down visual attention, three major sources of top-down influences have been explored, such as global scene context (Torralba et al., 2006; Peters and Itti, 2007), object features (appearance) (Kanan et al., 2009; Gao et al., 2009; Ehinger et al., 2009; Elazary and Itti, 2010; Rao et al., 2002; Lee et al., 2002), and task demands (Triesch et al., 2003; Navalpakkam and Itti, 2005). In the contextual guidance model (Torralba et al., 2006), local features, global features (scene gist), and object locations were integrated, and visual saliency was defined by the probability of the local features in the scene based on the scene gist. The gist was used to select relevant image regions for exploration. In classical search

Xu J..
Hierarchical Bayesian Modelling of Visual Attention.
DOI: 10.5220/0004731303470358
In *Proceedings of the 9th International Conference on Computer Vision Theory and Applications* (VISAPP-2014), pages 347-358
ISBN: 978-989-758-003-1

tasks, target features are a ubiquitous source of attention guidance (Einhauser et al., 2008). For complex target objects in natural scenes, there are other features that can drive visual attention. In (Kanan et al., 2009), an appearance-based saliency model was derived in a Bayesian framework. Responses of filters derived from natural images using independent component analysis (ICA) were used as the features. In (Rao et al., 2002), targets and scenes were represented as responses from oriented spatio-chromatic filters at multiple scales, and saliency maps were computed based on the similarity between a top-down iconic target representation and the bottom-up scene representation.

A prevailing view is that bottom-up and top-down attention is combined to direct our attentional behavior. An integration method should be able to explain when and how to attend to a top-down visual item or skip it for the sake of a bottom-up salient cue (Borji and Itti, 2013). In (Ehinger et al., 2009), computational models of search guidance from three sources, including bottom-up saliency, visual features of target appearance, and scene context, were investigated and combined by simple multiplication of three components. In (Zelinsky et al., 2006), the proportions of BU and TD components in a saliency-based model were manipulated to investigate top-down and bottom-up information in the guidance of human search behavior. In (Navalpakkam and Itti, 2007), the top-down component, derived from accumulated statistical knowledge of the visual features of the desired target and background clutter, was used to optimally tune the bottom-up maps such that the speed of target detection is maximized.

A hierarchical Bayesian inference model for early visual processing was proposed in (Lee and Mumford, 2003). In this framework, the recurrent feed-forward/feedback loops in the cortex serve to integrate top-down contextual priors and bottom-up observations, effectively implementing concurrent probabilistic inference along the visual hierarchy. It is well known that the sizes of the receptive fields of neurons increase dramatically as visual information traverses successive visual areas along the two visual streams (Serre et al., 2007; Tanaka, 1996)). For example, the receptive fields in V4 or the MT area are at least four times larger than those in V1 at the corresponding eccentricities (Gattass et al., 1988), and the receptive fields in the IT area tend to cover a large portion of the visual field. This dramatic increase in receptive-field sizes leads to a successive convergence of visual information necessary for extracting invariance and abstraction (e.g., translation and scaling), but it also results in the loss of spatial resolution and fine details in the higher visual areas (Lee and Mumford, 2003).

Inspired by the works of (Lee and Mumford, 2003) and the center-surround organization of receptive fields in the early visual cortex, we propose a hypothesis that neurons of the hierarchically organized visual cortex encode the conditional probability of observing visual variables in specific contexts.

To test this hypothesis, we developed a hierarchical Bayesian model of vision attention. We used a set of PDs based on the independent components (ICs) of natural scenes in a hierarchical center-surround configuration. The neurons at higher levels have larger receptive fields and lower resolutions, and provide local contexts to the neurons at lower levels. We estimated these PDs from natural scenes and derived measures of BU visual saliency and TD attention, which can be combined optimally. Finally, we conducted an extensive evaluation of this model and found that it is a good predictor of human fixations in free-viewing and object-searching tasks.

2 HIERARCHICAL BAYESIAN MODELING OF VISUAL ATTENTION

An input image is subsampled into a Gaussian pyramid. The original image at scale 0 has the finest resolution, and the subsampled image at the top scale has the coarsest resolution. At any location in an image, we sample a set of image patches of size N*N pixels at all levels of the pyramid. The local feature at scale s is denoted as F_s. In this pyramid representation, the feature at the scale $s+1$ is the context of the feature at scale s (C_s), as shown in Fig.1. Thus, the nodes in the higher levels have lower resolutions and larger receptive fields than the nodes in the lower levels, and provide the context for the features of the nodes in the lower levels. It should be pointed out that the contextual patch and object context are different; C_s is the contextual patch of F_s , which may or may not include the object context. Generally, the contextual patches at higher levels are more probable to cover some object context, and a contextual patch at a lower level just has object features, as shown in Fig.1. By using the hierarchical center-context structure, both object and its context features are supposed to be included. The knowledge of a target object O and its context includes appearance features at all scales F_i and location X . Assume that the distribution of object features does not change with spatial locations, then

$$P(F_0,F_1,\dots,F_n,X) = P(F_0,F_1,\dots,F_n)P(X). \quad (1)$$

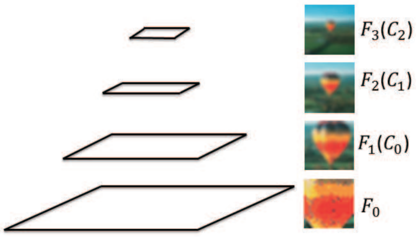

Figure 1: Image pyramid (left) and center-context configuration (right). The node at a higher level provides local context for the node at a lower level.

Given the features at location X the probability of the target object can be calculated as follows:

$$P(O|F_0,F_1,\ldots,F_n,X) = \frac{P(O,F_0,F_1,\ldots,F_n,X)}{P(F_0,F_1,\ldots,F_n,X)}$$

$$= \frac{1}{P(F_0,F_1,\ldots,F_n)} P(F_0,F_1,\ldots,F_n|O)P(O|X) \quad (2)$$

This entails the assumption that the distribution of a target feature is independent of spatial locations, i.e.,

$$P(F_0,F_1,\ldots,F_n|O,X) = P(F_0,F_1,\ldots,F_n|O). \quad (3)$$

The first term on the right side of equation (2),$1/P(F_0,F_1,\ldots,F_n)$, depends only on the visual features of all scales observed at the location, which is independent of the object, and therefore it is a bottom up factor and provides a measure of how unlikely it is to find a set of local measurements in natural scenes. This term fits the definition of saliency, and is the bottom-up saliency measure we use in this paper. The second term,$P(F_0,F_1,\ldots,F_n|O)$, represents the top-down knowledge of the target appearance. Regions of the input image with features unlikely to belong to the target object are vetoed and regions with attended features are enhanced. The third term,$P(O|X)$, is independent of visual features and reflects the prior knowledge of where the target is likely to appear. Next, we will describe each term in detail.

2.1 Bottom-up Attention

The bottom-up attention (saliency) is defined by the probability of observing visual variables in natural scenes. Saliency should be high for a rare visual variable, but low for a frequently occurring visual variable.

$$\frac{1}{P(F_0,F_1,\ldots,F_n)} = \frac{1}{P(F_0|F_1)} \cdots \frac{1}{P(F_{n-1}|F_n)} \frac{1}{P(F_n)} \quad (4)$$

Here we assume that the multi-scale features are a Markov chain, that is, given the features at the $(i+1)$-scale, the features at the i-th scale are independent on the features above the $(i+1)$-scale. The bottom-up saliency is given as

$$\begin{aligned} S_{MS}^{BU} &= \log \frac{1}{P(F_0,F_1,\ldots,F_n)} \\ &= -\log P(F_0|F_1) - \cdots - \log P(F_n) \quad (5) \end{aligned}$$

It is based on the features at all scales, therefore we use the notation S_{MS}^{BU}, where the low subscript means Multi-Scale, and the upper subscript means Bottom-Up. The multi-scale bottom-up saliency can be decomposed into saliency at each scale, and the bottom-up saliency at a single scale is defined as:

$$S_{SC}^{BU} = \log \frac{1}{P(F,C)} = -\log P(F|C) - \log P(C) \quad (6)$$

Here the feature at the $(i+1)$-th scale, F_{i+1} , serves as the context of the i-th scale, C_i. The first term is the saliency measured by the center feature in a given context, and the second term measured by the context. Note that similar saliency measures were used in previous works. In (Bruce and Tsotsos, 2009; Zhang et al., 2008; Torralba et al., 2006), the saliency measure was defined as $-\log P(F)$, which is equivalent to the second term in (6) and the PD was computed from a single image the subject is seeing (Bruce and Tsotsos, 2009; Torralba et al., 2006) or from a set of natural scenes (Zhang et al., 2008). In (Xu et al., 2010), the saliency measure was defined as $-\log P(F|C)$, where the context was the annular patch around the circular center. This measure is equivalent to the first term in (6). In this paper, a multi-scale bottom up saliency (5) is proposed, which can be regarded as the combination of visual saliency at all scales of the pyramid representation of an input scene. It can be seen that some saliency measures in the previous works are included in this model.

2.2 Top-down Attention

Top-down attention is based on the knowledge of the target and its context.

$$\begin{aligned} &P(F_0,F_1,\ldots,F_n|O) \\ &= P(F_0|F_1,O)\ldots P(F_{n-1}|F_n,O)P(F_n|O) \quad (7) \end{aligned}$$

Here we assume the target features at the i-th scale are only dependent on the features at the $(i+1)$-scale. The multi-scale top-down attention is then defined as:

$$\begin{aligned} S_{MS}^{TD} &= \log P(F_0,F_1,\ldots,F_n|O) \\ &= \log P(F_0|F_1,O) + \cdots + \log P(F_n|O) \quad (8) \end{aligned}$$

Similarly, the multi-scale TD attention can be decomposed into single scale attentions, and the TD attention at a single scale is defined as:

$$S_{SC}^{TD} = \log P(F,C|O) = \log P(F|C,O) + \log P(C|O) \quad (9)$$

The first term in (9) is the top-down attention measured by the center feature in a given context of the target. For regions in the image with features likely to belong to the target, it will have a higher value. The second term in (9) is the top-down attention measured by the context of the target.

In some previous top-down attention models, knowledge of target appearance was used. In (Elazary and Itti, 2010), $P(F|O)$ was defined as the top-down saliency, and all features from different channels and scales were assumed to be statistically independent from each other to simplify the computation. This is equivalent to replacing (7) by

$$\begin{aligned} & P(F_0, F_1, \cdots, F_n|O) \\ & = P(F_0|O) \cdots P(F_{n-1}|O) P(F_n|O) \end{aligned} \tag{10}$$

The PD was modeled by a Gaussian distribution independently. As discussed in (Elazary and Itti, 2010), features from different scales are unlikely to be statistically independent. In this paper, we will model the conditionally probability $P(F_i|O)$ and $P(F_i|F_{i+1}, O)$ explicitly.

2.3 Model of Object Location

In this paper, an object is represented by a set of local features, and the local features can be assumed to be independent of the object locations in input scenes. The object location attention is

$$S^{LOC} = \log P(O|X) \tag{11}$$

Under the assumption that $P(X)$ is uniformly distributed and $P(O)$ is constant for any specific object-search task, we have

$$P(O|X) = \frac{P(O,X)}{P(X)} \propto P(X|O) \tag{12}$$

The distribution of object locations is modeled by a Gaussian PD.

$$P(X|O) = N(X; \mu, \sigma) \tag{13}$$

The mean and variance of the object locations are estimated from the objects in training images. In (Torralba et al., 2006), a holistic representation of the scene (the gist) was used to guide attention to locations likely to contain the target, and then the top-down knowledge of an object location in a particular scene was combined with basic bottom-up saliency. By integration of the scene gist into our model, the location attention in (Torralba et al., 2006) can be easily embedded into our model.

$$S^{LOC} = \log P(O|X, G) \tag{14}$$

Where G is the scene gist. In the experiments in Section 4, we did not integrate the scene gist, and still use the location attention based on (11), since the goal of this paper is to propose a multi-scale framework which can combine the BU saliency and TD attention of object appearance and location.

2.4 Integration of Bottom-up and Top-down Attention

From Eq.(2), the full hierarchical Bayesian model of visual attention is given as:

$$\begin{aligned} S_{MS}^{FULL} &= \log \frac{P(F_0, F_1, \ldots, F_n|O)}{P(F_0, F_1, \ldots, F_n)} P(O|X) \\ &= S_{MS}^{BU} + S_{MS}^{TD} + S^{LOC} \end{aligned} \tag{15}$$

The first two terms are based on the multi-scale features (appearance), and can be decomposed as:

$$\begin{aligned} S_{MS}^{BUTD} &= S_{MS}^{BU} + S_{MS}^{TD} \\ &= \log \frac{P(F_0, F_1, \ldots, F_n|O)}{P(F_0, F_1, \ldots, F_n)} \qquad (16) \\ &= \log \frac{P(F_0|F_1, O)}{P(F_0|F_1)} + \cdots + \log \frac{P(F_n|O)}{P(F_n)} \end{aligned}$$

The single-scale appearance saliency can be defined as:

$$S_{SC}^{BUTD} = \log \frac{P(F|C,O)}{P(F|C)} + \log \frac{P(C|O)}{P(C)} \tag{17}$$

The first term is the saliency measured by the center feature in a given context, and the second term measured by the context.

There have been some attempts to integrate both top-down and bottom-up attention in the literature. In (Kanan et al., 2009), the top-down saliency was defined as, $P(O|F)$, and a probabilistic classifier was used to model this PD. This is equivalent to the second term in (17). In (Zelinsky et al., 2006), the proportions of BU and TD components in a saliency-based model were manipulated to investigate top-down and bottom-up information in the guidance of human search behavior. The weights of BU and TD components were tuned manually and there were no cues on how to tune the parameters. In this paper, the full attentional measure is the summation of BU and TD attentions, and there are no parameters to be tuned.

3 OBJECT REPRESENTATION AND IMPLEMENTATION

In this section, we will introduce the features used in this paper and the implementation of the proposed hierarchical Bayesian model.

3.1 Natural Scene Statistics and Object Representation

The features used here are the ICs of natural scenes. When ICA is applied to natural images, it yields filters qualitatively resembling those found in visual cortex (Olshausen and Field, 1996; Bell and Sejnowski, 1997). To obtain object features, we performed ICA on image patches drawn from the McGill calibrated color image database using the FastICA algorithm (Hyvarinen, 1999). We sampled a large number of scene patches (220,000) using the center-context configuration. Each sample is a set of patches at all the selected scales at the same position. The patch size at all scales was 21x21 pixels. We whitened the input data before running ICA and then reduced the dimensionality of the patches from 21*21*3= 1323 to 100 by selecting the most significant principal components. The ICs of the context was obtained using the FastICA algorithm:

$$C = A_C U_C \tag{18}$$

Here A_C is the mixing matrix and U_C is the ICA coefficient vector. The PDs of the context is

$$P(C) \propto P(U_C) = \prod_k u_C^k \tag{19}$$

To calculate the conditional PD $P(F|C)$, we used a modified FastICA algorithm to perform the ICA in Eq.(20) to achieve statistical independence within and between the components of U_C and U_F.

$$\begin{bmatrix} C \\ F \end{bmatrix} = \begin{bmatrix} A_C & 0 \\ A_{CF} & A_F \end{bmatrix} \begin{bmatrix} U_C \\ U_F \end{bmatrix} \tag{20}$$

Each column of A_C is a basis of the context C. Each column of A_{CF} is a basis of the center F, paired with a basis of the context. Each column of A_F is an unpaired basis of the center F. As shown in Figure.2, each paired basis of the center matches the center of the corresponding basis of the context, and each of these three sets has chromatic and achromatic basis.

The joint PDs of a center and its context is

$$P(C,F) \propto P(U_C)P(U_F) = \prod_k u_C^k \prod_k u_F^k \tag{21}$$

Here u_C^k, u_F^k are the k-th elements of U_C and U_F respectively. The conditional PDs, $P(F|C)$, can be derived using the Bayesian formula as follows:

$$P(F|C) = \frac{P(F,C)}{P(C)} = \frac{P(U_F)P(U_C)}{P(U_C)} \propto \prod_k u_F^k \tag{22}$$

For notational simplicity, we use c^k to denote the k-th context feature u_C^k and f^k for the center feature u_F^k.

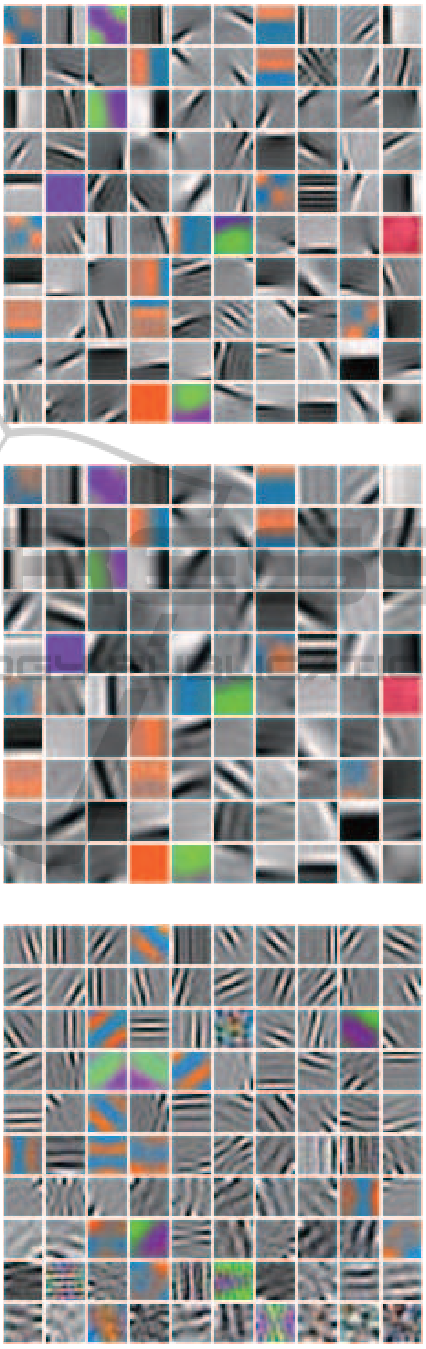

Figure 2: ICA basis of the context C and center F. Top: ICs of the context (columns of A_C in (20)). Middle: Paired ICs of the center (columns of A_{CF} in (20)). Each IC matches the center of the corresponding IC in (A). Bottom: Unpaired ICs of the center (columns of A_F in (20)). Each of these three sets has chromatic and achromatic ICs.

Due to the statistical independence, we only need to model each element (feature) for context C and for the center F from now on. Thus, the terms $\log P(C)$ and $\log P(F|C)$ can be calculated as follows:

$$\log P(C) = \sum_k \log P(c^k) \tag{23}$$

$$\log P(F|C) = \sum_k \log P(f^k) \tag{24}$$

Similarly, $P(C|O)$ and $P(F|C,O)$ can be calculated from the patches extracted on the target. The single-scale saliency measure in (17) is derived as follows:

$$\begin{aligned} S_{SC}^{BUTD} &= \log P(F|C,O) - \log P(F|C) \\ &+ \log P(C|O) - \log P(C) \\ &= \sum_k (\log P(f^k|O) - \log P(f^k)) \\ &+ \sum_k (\log P(c^k|O) - \log P(c^k)) \end{aligned} \tag{25}$$

We modeled the probability distribution $P(f|O)$, $P(f)$, $P(c|O)$ and $P(c)$ in (25) as generalized Gaussian distributions (GGD).

4 RESULTS

In this section, we test the models performance of human gaze prediction in free-viewing and object search tasks.

4.1 Free Viewing

We used the gaze data in free-viewing static color natural scenes collected by Bruce and Tsotsos (Bruce and Tsotsos, 2009) to evaluate our model of visual saliency. This dataset contains human gaze collected from 20 participants in free-viewing 120 color images of indoor and outdoor natural scenes.

To quantitatively access how well our model of visual saliency predicts human performance, we used the receiver operating characteristic (ROC) and the KullbackCLeibler (KL) divergence measure. To avoid a central tendency in human gaze (Zhang et al., 2008), we used the measure described in (Tatler et al., 2005). Rather than comparing the saliency measures at attended locations in the current scene to the saliency measures at unattended locations in the same scene, we compared the saliency measures at the attended locations to the saliency measures in that scene at the locations that are attended in different scenes in the dataset, called shuffled fixations.

Our model of visual saliency is a good predictor of human gaze during the free-viewing of static natural scenes, outperforming all other models that we tested. As shown in Table 1, our model has an average KL divergence of 0.3495 and its average ROC measure is 0.6863. The average KL divergence and ROC measure for the AIM model in (Bruce and Tsotsos, 2009) are 0.2879 and 0.6799 respectively, which were calculated using the code provided by the authors.

Table 1: ROC metric and KL-divergence for BU saliency of static natural scenes.

Model	KL	ROC
(Itti et al., 1998)	0.1130	0.6146
(Gao and Vasconcelos, 2007)	0.1535	0.6395
(Zhang et al., 2008)	0.1723	0.6570
(Bruce and Tsotsos, 2009)	0.2879	0.6799
(Xu et al., 2010)	0.3016	0.6803
S_{MS}^{BU}	0.3495	0.6863

4.2 Visual Search Tasks

We used the human data described in (Torralba et al., 2006) for visual search tasks. For completeness, we give a brief description of their experiment. Twenty-four Michigan State University undergraduates were assigned to one of three tasks: counting people, counting paintings, or counting cups and mugs. In the cup and painting counting groups, subjects were shown 36 indoor images (the same for both tasks), and in the people-counting groups, subjects were shown 36 outdoor images. In each of the tasks, targets were either present or absent, with up to six instances of the target appearing in the present condition. Images were shown until the subject responded with an object count or for 10s, whichever came first. Images, subtending $15.8^o \times 11.9^o$, were displayed on an NEC Multisync P750 monitor with a refresh rate of 143 Hz. Eyetracking was performed using a Generation 5.5 SRI Dual Purkinje Image Eyetracker with a sampling rate of 1000 Hz, tracking the right eye.

The training of top-down components of our model was performed on a subset of the LabelMe dataset (Russell et al., 2008). We used 198 images with cups/mugs, 426 images with paintings, and 389 images of street scenes for training. For testing, we used the stimuli sets shown to human subjects in Torralba et al's experiment.

We obtained 447 cups/mugs, 818 paintings, and 1357 people in the labeled training images. For each target object, we sampled a set of 21x21 patches from the images. Each set of patches includes patches at the same location at all the selected scales. For 21x21 patch size, we used only 3 scales. We sampled at most 3*3 sets of patches for a cup, 5*5 sets for a painting, and 2*5 sets for a person. We also sampled the same number of sets of negative patches from the background in the training images. We obtained the

PDs, $P(C)$ and $P(F|C)$, from the negative patches, and $P(C|O)$ and $P(F|C,O)$ from the object patches.

We obtained the object locations from the center of masks in the annotation data, and estimated $P(X|O)$ for each object category. As discussed in (Torralba et al., 2006), the horizontal locations of objects can be modeled by a uniformly distribution. Therefore, we only used the Gaussian distribution to model the vertical locations for each object category. The PDs of the object locations in the training images are shown in Fig.3. It was observed that cups are more likely to be in the middle of the images, paintings appear more frequently on the upper part of the images, and people on the lower part of the images. It should be pointed out that we focused on appearance of targets and contexts and used a simple model for the object location. In (Torralba et al., 2006), scene gist was used to model the distribution of object locations in specific input image. As discussed in Section 2.3, the location attention in (Torralba et al., 2006) can also be integrated into our model.

Fig.4 shows several saliency maps and the top 30% most salient regions for the test images used in the people search task. The saliency maps were smoothed using a Gaussian kernel with a half-amplitude spatial width of 1^o of visual angle, the same procedure used in (Kanan et al., 2009; Torralba et al., 2006) to make comparison with the density maps of human fixations. The first 5 fixations for all 8 subjects were superimposed on the original images (left column) and the selected regions (right column). As shown in Fig.4, most of human fixations fell into the top 10% most salient regions.

In Fig.5, we compared the saliency maps of the same images for different tasks. The bottom-up saliency map is same for both tasks. The top-down effects of the targets on the saliency maps were shown in the full saliency map and the selected top 30% most salient regions. As predicted by our model, the paintings became more salient in the painting search task and the mugs became more salient in the mug search task.

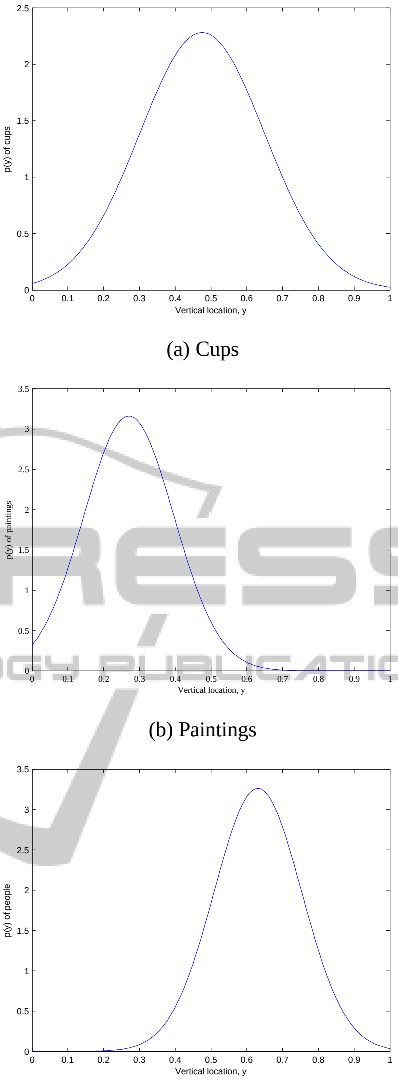

(a) Cups

(b) Paintings

(c) People

Figure 3: Distribution of the normalized vertical locations of objects.(0 means top; 1 means bottom.)

To examine how well the hierarchical model proposed here predicts human fixations quantitatively, we adopted the performance measure used in (Torralba et al., 2006) and (Kanan et al., 2009). The measure evaluates the percentage of each subjects first five fixations being made to the top 20% most salient regions of the saliency map. The fixation prediction rates for the three object search tasks were shown in Table 2. For comparison, the results in (Torralba et al., 2006) were also shown in Table 2, these data were read from the figures in their paper. It can be seen that the BU saliency measure of our model is similar or better than that in (Torralba et al., 2006) for all three tasks. For the full model, our result is better in painting tasks, but not as good as the results in (Torralba et al., 2006) for mug and people search tasks. This is because the low-level object features are used at all scales, the contexts at higher scales are too coarse and abstract to be discriminative, therefore for complex objects like pedestrians, the appearance model is not powerful enough. For small objects like cups and mugs, the contexts at higher scales are most from backgrounds, not from objects.

To investigate the effects of patch sizes and scales on the performance, we re-ran the model using image patches of 11 × 11 pixels at 4 scales. The results for different patch sizes were similar, with about

Table 2: Performance comparison in object search tasks. PR (PresentRate) is for images with target present, AR (AbsentRate) for images with target absent. Average is the average of PR and AR. CGM is the context-guidance model in (Torralba et al., 2006)

Tasks	Models	PR	AR	Average
Painting	BU(CGM)	0.42	0.44	0.43
	S^{BU}_{MS}	0.47	0.43	0.45
	CGM	0.57	0.48	0.53
	S^{FULL}_{MS}	0.63	0.51	0.57
Mug	BU(CGM)	0.71	0.62	0.66
	S^{BU}_{MS}	0.70	0.61	0.65
	CGM	0.82	0.65	0.74
	S^{FULL}_{MS}	0.74	0.64	0.69
People	BU(CGM)	0.63	0.49	0.56
	S^{BU}_{MS}	0.67	0.51	0.59
	CGM	0.78	0.65	0.72
	S^{FULL}_{MS}	0.71	0.58	0.64

2% improvement on the average rate for patch size of 11×11 at 4 scales.

We also tested the performance of various saliency measures proposed in Section 2. Due to page limitations, we show the results of 6 selected measures in Table 3 to Table 5 for the visual search tasks. These results show several important aspects of the model proposed here. 1), all saliency measures make better predictions than the location measure only. 2), the bottom-up saliency measures make good predictions since the targets (e.g., cups, paintings, and people) are usually salient. 3), the multi-scale saliency measures are better than single-scale measures. 4), the measure with TD and BU integrated are better than the bottom-up only measure.

The results in Table 2 and Table 3 to Table 5 also show several weaknesses of the current implementation of our model. First, the Gaussian PD model of object locations is weak in some cases. For the mug search task, the location saliency is slightly higher than the chance level, 20%. Therefore the integration of the location saliency into the full model does not make any improvement. This may be because there were only 447 mugs/cups in the training images. For the people search task, there were 1357 people in the training images, and the location measure performs better (45% average rate). If the object location distribution is estimated by the scene gist, as implemented in (Torralba et al., 2006), the full model should have better performance. Second, the low-level object features are not sufficiently discriminative with respect to the backgrounds. As a result, the contribution of the top-down attention was less than the bottom-up saliency. In future works, we will include intermediate and high-level object features and develop more powerful models of object locations in natural contexts.

Table 3: Performance of saliency models in predicting human gaze for the painting search task.

Measure	PR	AR	Average
S^{LOC}	0.3644	0.3208	0.3426
S^{BU}_{SC0}	0.4648	0.4267	0.4458
S^{BU}_{SC1}	0.4605	0.4023	0.4314
S^{BU}_{SC2}	0.4032	0.4137	0.4084
S^{BU}_{MS}	0.4663	0.4332	0.4498
S^{BUTD}_{SC0}	0.4577	0.4593	0.4548
S^{BUTD}_{SC1}	0.4548	0.3811	0.4180
S^{BUTD}_{SC2}	0.4075	0.2997	0.3536
S^{BUTD}_{MS}	0.5681	0.4137	0.4909
S^{FULL}_{MS}	0.6298	0.5147	0.5723

Table 4: Performance of saliency models in predicting human gaze for the mug search task.

Measure	PR	AR	Average
S^{LOC}	0.2463	0.2138	0.2300
S^{BU}_{SC0}	0.6634	0.5948	0.6291
S^{BU}_{SC1}	0.6894	0.6138	0.6516
S^{BU}_{SC2}	0.6584	0.5724	0.6154
S^{BU}_{MS}	0.6955	0.6138	0.6547
S^{BUTD}_{SC0}	0.6869	0.5810	0.6340
S^{BUTD}_{SC1}	0.7042	0.6345	0.6693
S^{BUTD}_{SC2}	0.6844	0.5897	0.6370
S^{BUTD}_{MS}	0.7438	0.6448	0.6943
S^{FULL}_{MS}	0.7438	0.6397	0.6917

5 CONCLUSIONS

We made three contributions in this paper. First, we proposed a biologically inspired, hierarchical Bayesian model of visual attention. We used multi-

Table 5: Performance of saliency models in predicting human gaze for the people search task.

Measure	PR	AR	Average
S^{LOC}	0.5512	0.3498	0.4505
S^{BU}_{SC0}	0.6042	0.4778	0.5410
S^{BU}_{SC1}	0.6609	0.4915	0.5762
S^{BU}_{SC2}	0.6732	0.4898	0.5815
S^{BU}_{MS}	0.6708	0.5102	0.5905
S^{BUTD}_{SC0}	0.5536	0.4283	0.4910
S^{BUTD}_{SC1}	0.6449	0.5171	0.5810
S^{BUTD}_{SC2}	0.6967	0.5171	0.6069
S^{BUTD}_{MS}	0.6905	0.5512	0.6209
S^{FULL}_{MS}	0.7127	0.5751	0.6439

scale features and modeled conditional PDs of these features to measure TD and BU visual saliency. We optimally combined top-down attention and bottom-up visual saliency in a Bayesian framework. Second, we showed that the model can predict human fixations very well in free viewing and object searching tasks. Finally, we obtained a range of useful observations on top-down attention, bottom-up saliency, visual search, object detection, and the effects of visual context.

These results support the hypothesis that neurons in the visual cortex may act as estimators of the conditional PDs of visual features in specific contexts in natural scenes and the visual features are encoded progressively downward the hierarchical visual cortex. An ongoing debate in current studies on visual saliency is whether or not there should be a saliency map in the brain. In our model, computational units of the hierarchically organized visual system encode the conditional PDs of visual variables in natural contexts and thus convey saliency information explicitly. Therefore, no further complicated operations are needed to calculate visual saliency and the visual saliency may distribute at all levels of the visual cortex.

In the pioneering bottom up saliency model (Itti et al., 1998), multi-scale features were also used, as in our model. Although both models are biologically inspired, our model is different from theirs in the following ways. First, in (Itti et al., 1998), center-surround differences between a center at a finer scale and a surround at a coarser scale yield the feature maps. In our model, the saliency measure was defined based on the conditional probability distribution of a center in a surround (context). Second, we used independent components learned from natural scenes, whereas in (Itti et al., 1998), orientation, color and intensity features were used. The SUN model in (Kanan et al., 2009) is most related to our work. In SUN model, the PD $P(O|F)$ was modeled using SVM, therefore it is a discriminative approach, different from our generative model, in which $P(F|O)$ is modeled using GGD. Meanwhile, our model has multi-scale hierarchical architecture, different from the single scale in SUN.

ACKNOWLEDGEMENTS

This work is supported by the National Natural Science Foundation of China under Project 61175116, and Shanghai Knowledge Service Platform for Trustworthy Internet of Things (No. ZF1213).

REFERENCES

Bell, A. J. and Sejnowski, T. J. (1997). The ”independent components” of natural scenes are edge filters. *Vision Res*, 37:3327–38.

Borji, A. and Itti, L. (2013). State-of-the-art in visual attention modeling. *IEEE Trans Pattern Anal Mach Intell*, 35:185–207.

Bruce, N. D. and Tsotsos, J. K. (2009). Saliency, attention, and visual search: an information theoretic approach. *J Vision*, 9:1–24.

Ehinger, K. A., Hidalgo-Sotelo, B., Torralba, A., and Oliva, A. (2009). Modeling search for people in 900 scenes: A combined source model of eye guidance. *Visual Cognition*, 17:945–978.

Einhauser, W., Spain, M., and Perona, P. (2008). Objects predict fixations better than early saliency. *J Vis*, 8:1–26.

Elazary, L. and Itti, L. (2010). A bayesian model for efficient visual search and recognition. *Vision Res*, 50:1338–52.

Frintrop, S., Rome, E., and Christensen, H. I. (2010). Computational visual attention systems and their cognitive foundations: A survey. *ACM Transactions on Applied Perception*, 7:1–46.

Gao, D., Han, S., and Vasconcelos, N. (2009). Discriminant saliency, the detection of suspicious coincidences, and applications to visual recognition. *IEEE Trans Pattern Anal Mach Intell*, 31:989–1005.

Gao, D. and Vasconcelos, N. (2007). Bottom-up saliency is a discriminant process. In *ICCV*. IEEE.

Gao, D. and Vasconcelos, N. (2009). Decision-theoretic saliency: computational principles, biological plausibility, and implications for neurophysiology and psychophysics. *Neural Comput*, 21:239–71.

Gattass, R., Sousa, A. P., and Gross, C. G. (1988). Visuotopic organization and extent of v3 and v4 of the macaque. *Journal of neuroscience*, 8:1831–45.

Hyvarinen, A. (1999). Fast and robust fixed-point algorithms for independent component analysis. *IEEE Trans Neural Netw*, 10:626–34.

Itti, L. and Baldi, P. (2009). Bayesian surprise attracts human attention. *Vision Res*, 49:1295–306.

Itti, L., Koch, C., and Niebur, E. (1998). A model of saliency-based visual attention for rapid scene analysis. *IEEE Trans Pattern Anal Mach Intell*, 20:1254–1259.

Kanan, C., Tong, M. H., Zhang, L., and Cottrell, G. W. (2009). Sun: Top-down saliency using natural statistics. *Visual Cognition*, 17:979–1003.

Lee, T. S. and Mumford, D. (2003). Hierarchical bayesian inference in the visual cortex. *Journal of the Optical Society of America A, Optics, image science, and vision*, 20:1434–48.

Lee, T. S., Yang, C. F., Romero, R. D., and Mumford, D. (2002). Neural activity in early visual cortex reflects behavioral experience and higher-order perceptual saliency. *Nature neuroscience*, 5:589–97.

Navalpakkam, V. and Itti, L. (2005). Modeling the influence of task on attention. *Vision Res*, 45:205–31.

Navalpakkam, V. and Itti, L. (2007). Search goal tunes visual features optimally. *Neuron*, 53:605–17.

Olshausen, B. A. and Field, D. J. (1996). Emergence of simple-cell receptive field properties by learning a sparse code for natural images. *Nature*, 381:607–9.

Peters, R. J. and Itti, L. (2007). Beyond bottom-up: Incorporating task-dependent influences into a computational model of spatial attention. In *CVPR'06*. IEEE.

Rao, R. P., Zelinsky, G. J., Hayhoe, M. M., and Ballard, D. H. (2002). Eye movements in iconic visual search. *Vision Res*, 42:1447–63.

Russell, B. C., Torralba, A., Murphy, K. P., and Freeman, W. T. (2008). Labelme: A database and web-based tool for image annotation. *International Journal of Computer Vision*, 77:157–173.

Serre, T., Oliva, A., and Poggio, T. (2007). A feedforward architecture accounts for rapid categorization. *Proc Natl Acad Sci U S A*, 104:6424–9.

Tanaka, K. (1996). Inferotemporal cortex and object vision. *Annual review of neuroscience*, 19:109–39.

Tatler, B. W., Baddeley, R. J., and Gilchrist, I. D. (2005). Visual correlates of fixation selection: effects of scale and time. *Vision Res*, 45:643–59.

Toet, A. (2011). Computational versus psychophysical bottom-up image saliency: a comparative evaluation study. *IEEE Trans Pattern Anal Mach Intell*, 33:2131–46.

Torralba, A., Oliva, A., Castelhano, M. S., and Henderson, J. M. (2006). Contextual guidance of eye movements and attention in real-world scenes: the role of global features in object search. *Psychol Rev*, 113:766–86.

Triesch, J., Ballard, D. H., Hayhoe, M. M., and Sullivan, B. T. (2003). What you see is what you need. *J Vis*, 3:86–94.

Xu, J., Yang, Z., and Tsien, J. Z. (2010). Emergence of visual saliency from natural scenes via context-mediated probability distributions coding. *PLoS ONE*, 5.

Zelinsky, G. J., Zhang, W., Yu, B., Chen, X., and Samaras, D. (2006). The role of top-down and bottom-up processes in guiding eye movements during visual search. In *NIPS'06*. Cambridge, MA: MIT Press.

Zhang, L., Tong, H., Marks, T., Shan, H., and Cottrell, G. W. (2008). Sun: A bayesian framework for saliency using natural statistics. *J Vis*, 8:1–20.

APPENDIX

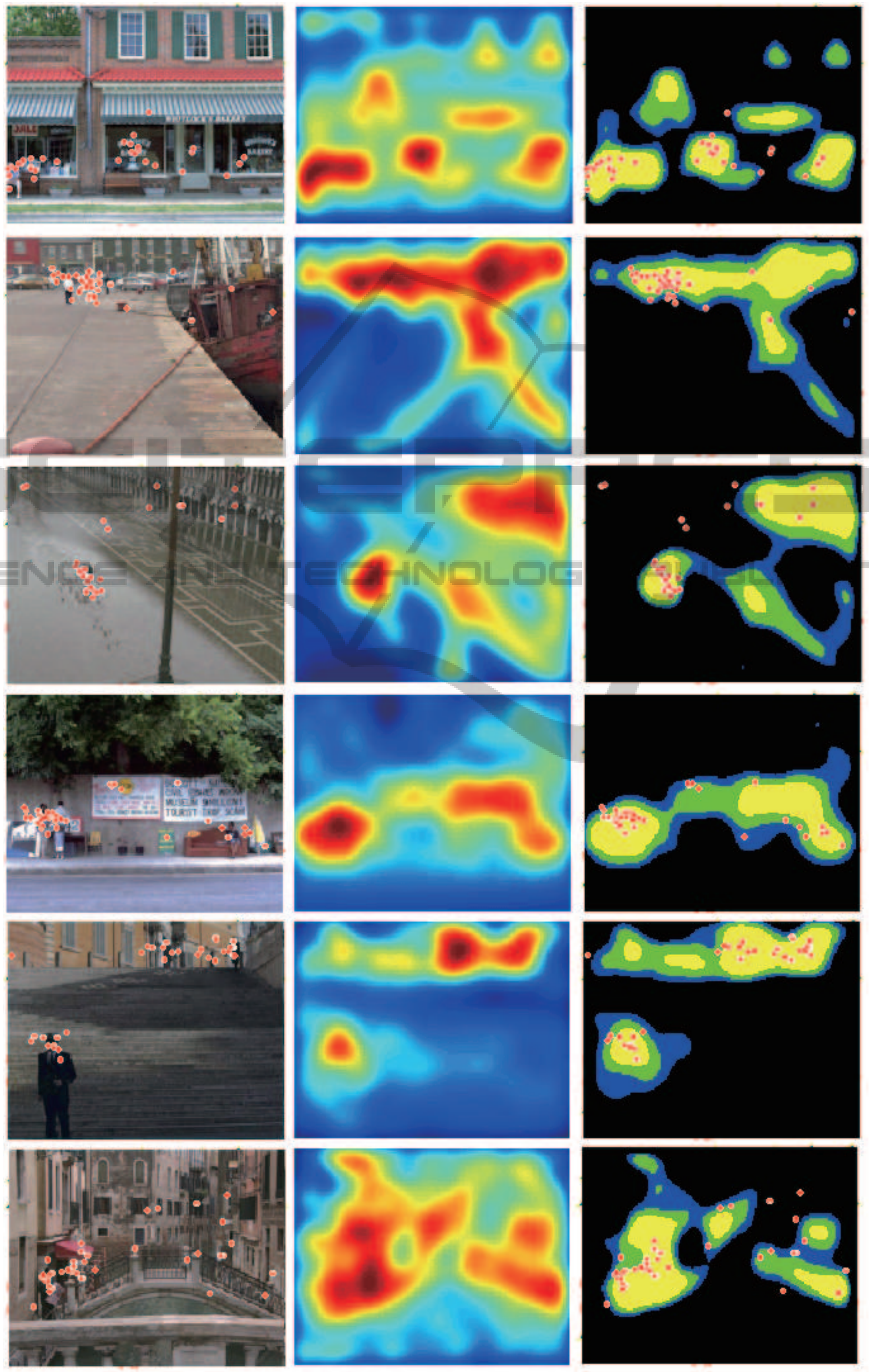

Figure 4: Saliency maps and selected regions for the people search task. Each panel shows the original images with the first 5 fixations for all 8 participants superimposed (left), the full saliency maps (middle), the top 30% most salient regions of the saliency maps with the subject fixations (right), where yellow, green, and blue correspond to the top 10, 20, and 30% most salient regions respectively.

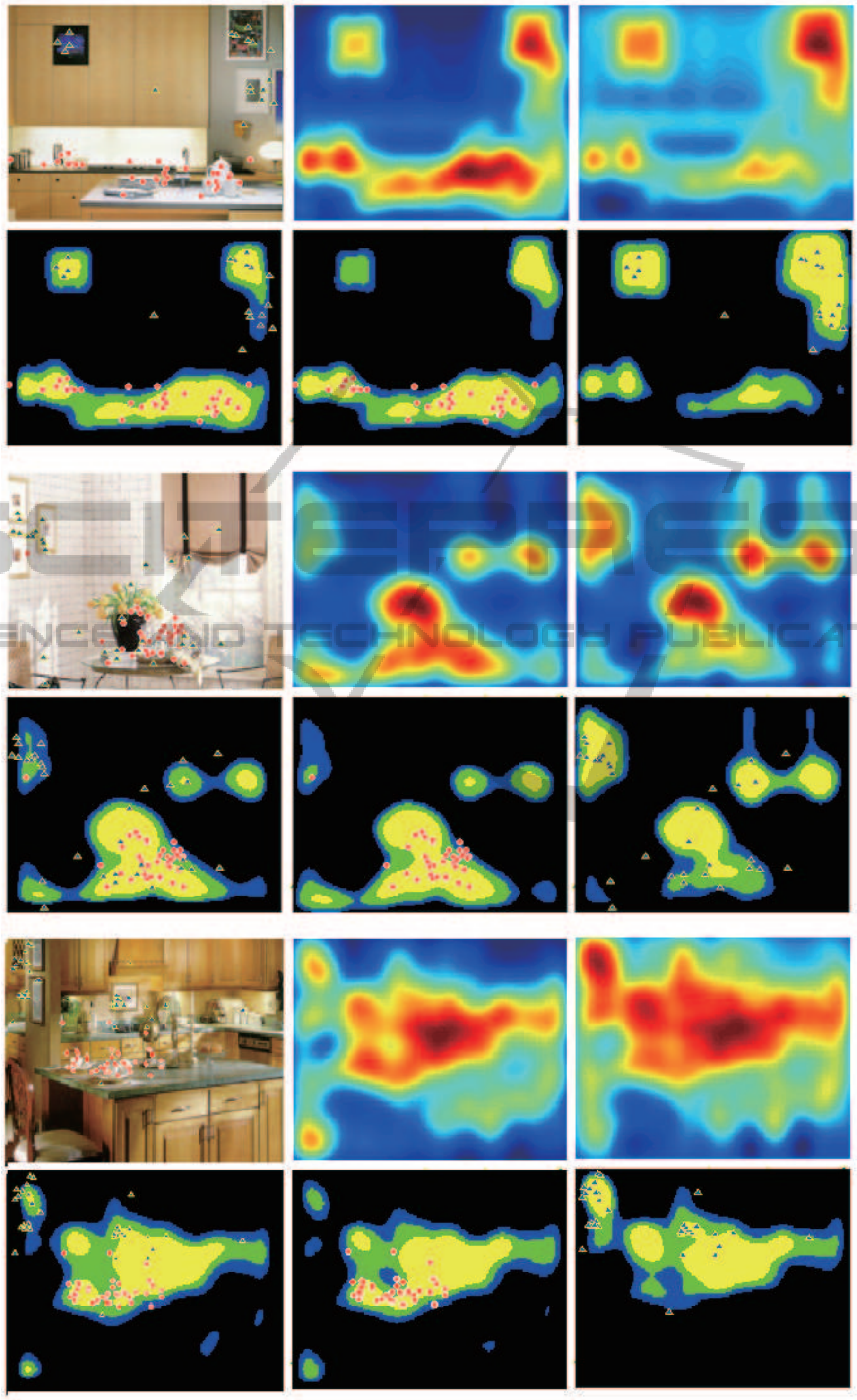

Figure 5: Saliency maps and selected regions for the mug and painting search tasks. The left column of each panel is the original image (top) and top 30% most salient regions from bottom-up saliency map (bottom) with the first 5 fixations for all subjects superimposed for both search tasks (red circles for mug search and blue triangles for painting search). The middle column is the full saliency map (top) and its top 30% most salient regions (bottom) for cup search task. The right column is the full saliency map (top) and its top 30% most salient regions (bottom) for painting search task.